Inside...
Visiting Fellows' Reports 2
Current Abstracts 3

The IRM Quarterly
Fall 1999, Vol. 9, No. 3 Institute for Rock Magnetism

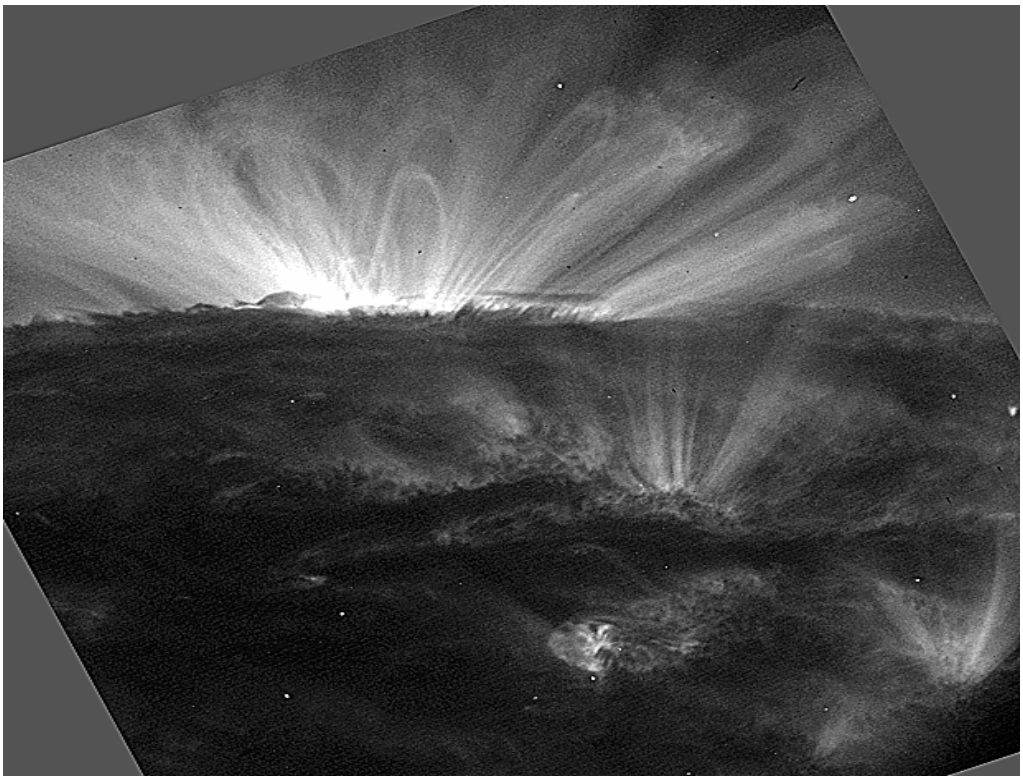

http://vestige.lmsal.com/TRACE/Public/Gallery/Images/

Ultraviolet emissions from highly ionized iron atoms (Fe^{9+}) reveal the detailed structure of solar magnetic fields. Ions spiral tightly around the magnetic field lines; bright areas show hot (1 million Kelvin) but dense magnetically-confined plasma.

Astronomical Magnetic Fields

Mike Jackson

IRM

The Earth's magnetic field is, admittedly, pretty weak. A mere 50 microtesla, it is quite inadequate, by itself, to make a lasting impression on rocks or sediments; natural magnetic recording is made possible only through the conspiracy of thermal, chemical, or physical processes. Of course, it is this very weakness that makes possible the preservation of paleomagnetic records in geological materials - if the field were too potent, it would continuously reset all previously imprinted magnetizations. However, our purpose here is not so much to praise the subtlety of the geomagnetic field, as to explore the opposite end of the "power" spectrum: how strong can magnetic fields be?

Certainly the field is greater in the Earth's core than at the surface. The poloidal component reaches at least 100 microtesla at the poles of the outer core (the poloidal component is the portion of the field oriented radially and/or north-south; this is the component we can measure at the surface) . The toroidal component (with field lines following circles of latitude, never leaving the core) is more mysterious, since it cannot be measured directly. Nevertheless, indirect evidence suggests an upper limit of about 5 millitesla (5000 microtesla) for the toroidal field in the core, 100 times the magnitude of the surface field.

We can do much better than that in the laboratory, albeit over much tinier spatial scales. Electromagnets (like those in our vibrating-sample magnetometers) routinely generate steady fields of 1 tesla or more. A major limitation on electromagnets is resistive dissipation of the current flowing in the wire coils; the heat generated is removed by a water circulation system. This limitation can be side-stepped either by eliminating the resistance of the coil (superconducting magnets), or by limiting the duration of the strong currents (pulse magnetizers). The superconducting magnets in our SQUID susceptometers maintain fields up to 5 tesla over the ≈6-mm-diameter bore of the instrument. Commercially-available pulse magnetizers can generate transient fields of several tesla (for a few milliseconds) by discharging a bank of capacitors through a solenoid.

The magnetic fields used in medical imaging are comparable to ours (OK, perhaps one notch above). Magnetic resonance imaging (MRI) makes use of the fact that protons in a magnetic field precess, or wobble, as they spin, with a precession frequency proportional to the magnetic field strength (this effect is also exploited in proton-precession magnetometers). The physics of MRI, though an interesting story in its own right, need not concern us here; suffice it to say that stronger magnetic fields are desirable, ultimately because they produce better resolution in the final images. Medical MRI instruments use superconducting magnets to apply at least 1 tesla over a volume large enough to enclose a human patient. The University of Minnesota's Center for Magnetic Resonance Research is home to a 7 tesla MRI system for whole-body imaging, and a smaller-volume 9.4 tesla system, representing the highest magnetic field currently used for human research. (Not to be outdone, the National High Magnetic Field Laboratory and the University of Florida Brain Institute have just acquired an 11.8 tesla MRI system with a 40-centimeter chamber.)

An efficient resistive (non-superconducting) magnet design worked out by Francis Bitter in the 1930's is still in wide use, generating steady fields comparable to and even exceeding those produced by superconducting magnets. The High Field Magnet Laboratory at the University of Nijmegen, a center for research in very high magnetic fields, features three superconducting magnets with fields up to 18.5 tesla, and three

Fields

continued on page 6...

H.F. Passier
Utrecht University
hpassier@geo.uu.nl

Magnetic Properties Around The Active Oxidation Front In Eastern Mediterranean Sediments

Traveling to the IRM in May, I carried almost 200 vials with powdered sediments with me from Utrecht to Minneapolis, definitely a sufficient amount to keep me busy for ten days. The main purpose of my stay was to measure low-temperature magnetic properties of eastern Mediterranean boxcore-sediments with the MPMS-5S. Earlier rock-magnetic measurements at room temperature and above yielded interesting results that warranted further exploration.

The boxcores contained the most recent Mediterranean organic-rich layer (sapropel Si2). The past and present diagenetic systems within and around this sapropel have been thoroughly studied from a geochemical perspective (van Santvoort et al., 1996; Passier et al., 1999). Anoxic sulfidic conditions during deposition of the sapropel from 5 to 9 kyr ago caused large scale reductive dissolution of iron oxides and pyritization in the sapropel and sediments directly below the sapropel. At present, an oxidation front is situated at the top of the organic-rich layer, dividing oxic surface sediments and underlying sediments that are currently suboxic. As a result of this oxidation, the sapropel becomes progressively thinner and the sediments immediately above the sapropel become enriched in iron oxides.

Earlier measurements with the Curie balance in air indicated that (maghemitized) magnetite, and possibly maghemite, magnetically dominate in the entire cores. Furthermore, ARM and IRM measurements at room temperature showed that the newly formed iron oxides above the sapropel carry a relatively high ARM, indicating the formation of SD to PSD grains. These oxides are highly coercive, especially in the cm-wide zone of active oxidation at the top of the sapropel. While the earlier measurements suggest some distinct sequence of formation and turnover of iron oxides after their precipitation at the front, magnetic analysis at room temperature and above could not satisfactorily clarify what particular phases formed subsequently.

Low-temperature magnetic measurements may provide more detailed information about the envisioned variations in grain size and mineralogy. Here we briefly summarize some of the most evident results of the performed LT SIRM (ZFC and FC), and RT SIRM measurements (Figure 1). The Verwey transition is clearly present around ~100 K in the sediments that have not been affected by diagenesis, while just above the sapropel and further down, this transition is absent. Unaltered sediments therefore contain stoichiometric magnetite grains, while all sediments below do not. This may indicate that the authigenic iron oxides are maghemitized. The iron oxides remaining after reductive dissolution within the sapropel and below may also be maghemitized as a result of preferential diffusion of Fe^{2+} out off the grains. Furthermore, at 20 K the FC remanence is higher than the ZFC remanence. The remanence curves converge during warming; the convergence temperature and the shapes of the curves vary consistently downcore. For example, the ratio of FC and ZFC remanences at 20 K is the highest in the oxidation front, and the convergence temperature is lower in the front (e.g. #76, Figure 1b). These downcore changes suggest subtle variations in grain-size distribution and mineralogy. Possibly the presence of defects in the magnetite crystal lattice may cause differences in FC and ZFC remanences, as suggested by Smirnov (1999) in his Visiting Fellows' Report on sediment samples from a Pacific redox boundary. We are presently working on the incorporation of the low-temperature results into the diagenetic model for the sapropel and the oxidation front. Thanks are due to all people at the IRM who made it possible to obtain these interesting results. I highly appreciated the stimulating discussions and their help in the laboratory. Supported by MAS3-CT97-0137 (SAP)

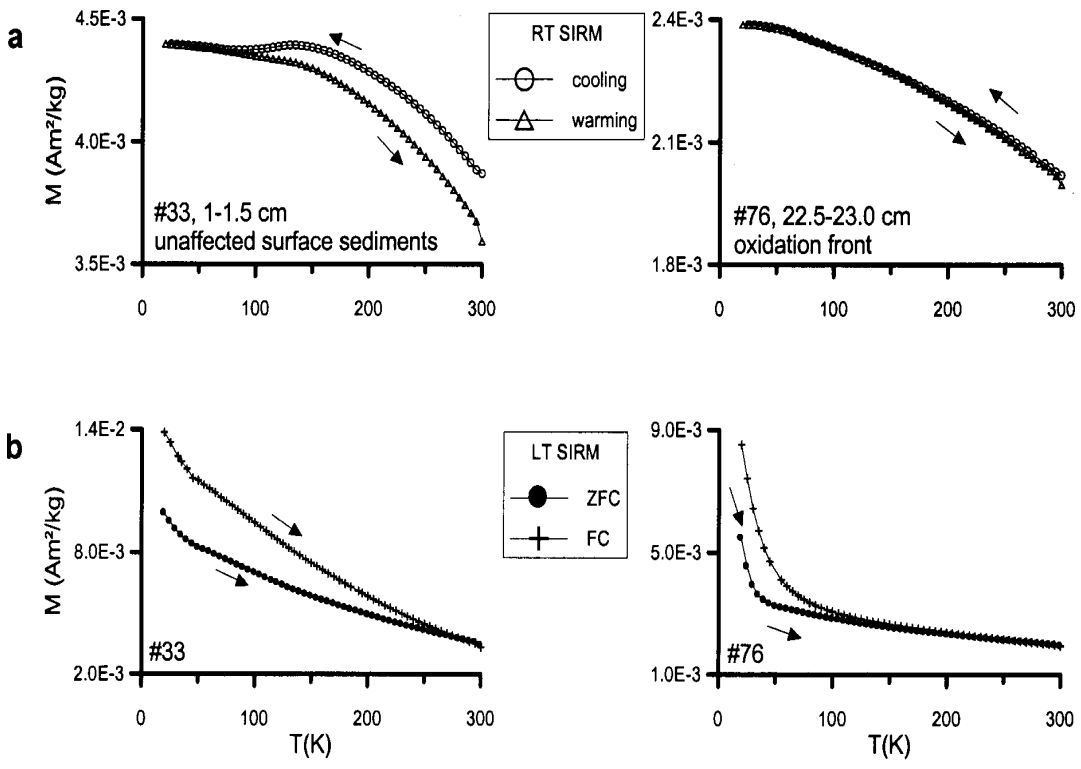

*Figure 1. Remanence curves for two eastern Mediterranean boxcore samples, #33 and #76, **a** measured during subsequent cooling and warming of an SIRM given at room temperature in 2.5T (RT SIRM), and **b** measured during warming of an SIRM given at 20K in 2.5T (LT SIRM) after cooling in absence of a field (zero field cooling, ZFC) and in presence of a field of 2.5T (field cooling, FC).*

References:

Passier, H. F. et al., *Mar. Geol.* **153**, 199-219, 1999.

Smirnov, A., *The IRM Quarterly* 9 (1), 2, 1999.

van Santvoort, P. J. M. et al., *Geochim. Cosmochim. Acta* **60**, 4007-4024, 1996.

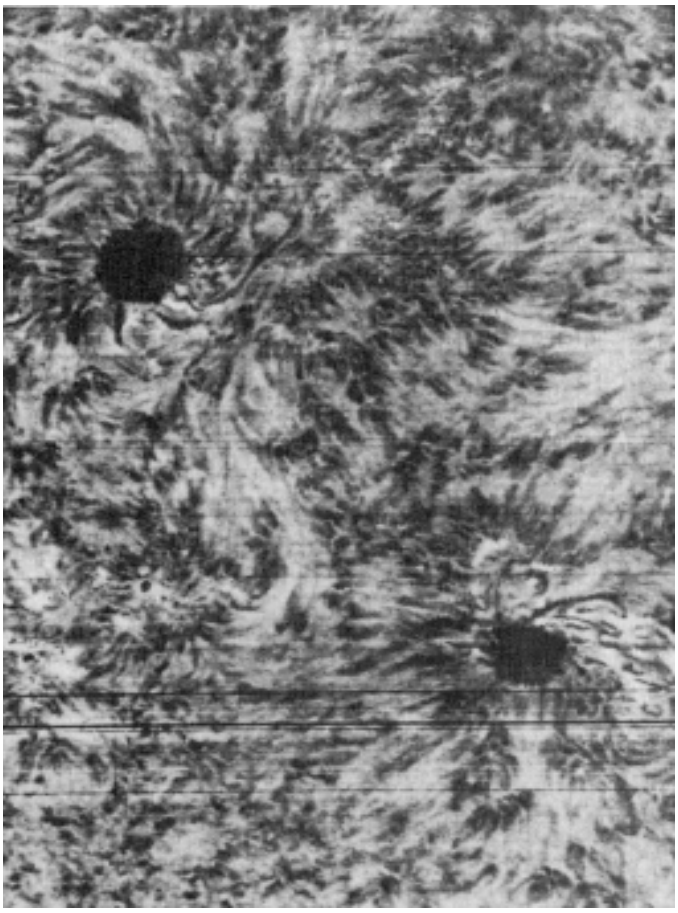

A dipolar magnetic sunspot pair at Hα hydrogen wavelength, imaged at Palomar, September 9, 1908. From ***Explorer of the Universe: A Biography of George Ellery Hale****, by Helen Wright. History of Modern Physics and Astronomy, v. 14, American Institute of Physics, 1994.*

Current Abstracts

A list of current research articles dealing with various topics in the physics and chemistry of magnetism is a regular feature of the IRM Quarterly. *Articles published in familiar geology and geophysics journals are included; special emphasis is given to current articles from physics, chemistry, and materials-science journals. Most abstracts are culled from* INSPEC *(© Institution of Electrical Engineers),* Geophysical Abstracts in Press *(© American Geophysical Union), and* The Earth and Planetary Express *(© Elsevier Science Publishers, B.V.), after which they are subjected to Procrustean editing and condensation for this newsletter. An extensive reference list of articles (primarily about rock magnetism, the physics and chemistry of magnetism, and some paleomagnetism) is continually updated at the* IRM. *This list, with more than 4200 references, is available free of charge. Your contributions both to the list and to the Abstracts section of the* IRM Quarterly *are always welcome.*

Environmental Magnetism and Paleoclimate

Jordanova, D., and Petersen, N., 1999, **Palaeoclimatic record from a loess-soil profile in northeastern Bulgaria. I. Rock magnetic properties**: *Geophysical Journal International, v. 138*, no. 2, p. 520-32.
Thermomagnetic analyses on bulk material suggest magnetite and maghemite as the main ferrimagnetic carriers in both soil and loess horizons. Chernozem soils, which include the recent soil S0 and palaeosols S1 and S2, developed under steppe vegetation and show a high degree of low-temperature oxidation of the pedogenic magnetite to maghemite. The older palaeosols (S4 to S6) were formed during more humid climatic conditions and therefore probably developed as forest types. Rock magnetic data suggest the existence here of only partly oxidized magnetite grains. The behaviour of the thermomagnetic curves, characterized by a kink at 200° C, may be due to either a release of internal stress (built up as a result of partial low-temperature oxidation) or interactions between two phases.

Kissel, C., Laj, C., Labeyrie, L., Dokken, T., Voelker, A., and Blamart, D., 1999, **Rapid climatic variations during marine isotopic stage 3: magnetic analysis of sediments from Nordic Seas and North Atlantic**: *Earth and Planetary Science Letters, v. 171*, no. 3, p. 489-502.
The bulk magnetic parameters of seven deep-sea cores exhibit short-term variations in ferrimagnetic content, which correlate with rapid climatic changes during MIS3. Variations in magnetic content are related to fast changes in the strength of the deep-sea circulation. The presence of magnetic oscillations in the Bermuda Rise core in phase with those from the North Atlantic indicates that the activity of the southern Newfoundland Basin gyre was linked to that of the NADW during MIS3.

Reinders, J., and Hambach, U., 1999, **Paleoenvironmental conditions in a travertine complex deduced from rock magnetism**: *Geophysical Research Letters, v. 26*, no. 15, p. 2267-70.
Concentration-dependent magnetic parameters and inter-parametric ratios point to varying redox conditions through time and space, suggesting local paleoenvironmental rather than paleoclimatic control of the rock magnetic properties.

Xiao-Min, F., Li, J.-J., Banerjee, S. K., Jackson, M., Oches, E. A., and Van der Voo, R., 1999, **Millennial-scale climatic change during the last interglacial period: superparamagnetic sediment proxy from paleosol S1, western Chinese Loess Plateau**: *Geophysical Research Letters, v. 26*, no. 16, p. 2485-8.
Low-temperature remanence studies show that the concentration of superparamagnetic (SP) grains exhibits millennial scale variations within the S1 paleosol. The last interglacial period in Asia was characterized by rapid climate fluctuations, with at least one brief return to near-glacial conditions in the middle of oxygen-isotope substage 5e.

Instruments and Measurements

Harrell, J. W., 1999, **Effect of AC gradient field on magnetic measurements with an alternating gradient magnetometer**: *Journal of Magnetism and Magnetic Materials, v. 205*, no. 1, p. 121-9.
The effect of the AC gradient field on measurements of the field dependence of magnetic viscosity and irreversible susceptibility has been examined both theoretically and experimentally. Two effects are predicted: (1) The AC field produces a change in the shape of the curves by an amount which is proportional to the product of the second derivative of the curve with respect to H and the square of the effective AC field over the sample. (2) The AC field induces magnetization reversal because of the nonlinear dependence of the relaxation rate on the applied field.

Harrison, S. A., Street, R., Budge, J. R., and Jones, S. K., 1999, **Rotational hysteresis losses in isotropic media**: *IEEE Transactions on Magnetics, v. 35*, no. 5, pt.2, p. 3962-4.
A simple method of measuring magnetic rotational hysteresis losses in isotropic media involves measuring the angular deceleration of a sample set rotating in a magnetic field. By using air bearings to minimise friction and allowing the moment of inertia of the rotating system to be varied, a maximum sensitivity of 10^{-6} J cycle^{-1} has been achieved with a precision of $3*10^{-7}$ cycle^{-1}.

Magnetic Field Behavior and Recording Mechanisms

Camps, P., Coe, R. S., and Prevot, M., 1999, **Transitional geomagnetic impulse hypothesis: geomagnetic fact or rock-magnetic artifact?**: *Journal of Geophysical Research, v. 104*, no. B8, p. 17747-58.
A paleomagnetic investigation of two new sections in the Steens summit region covers gaps in the previous study. The main result is the description of two new directions, which are located between the pre second and post second impulse directions. These findings weigh against the hypothesis that the geomagnetic field caused the unusual intraflow fluctuations. However, the alternative baking hypothesis remains ad hoc since one has to assume variable rock magnetic properties that have not yet been detected within the flows at the original section 1.5 km to the north.

Haag, M., Paterne, M., and Pujol, C., 1999, **Anomalous directions of the natural remanent magnetization in Late Pleistocene marine sediments from the coast of Mauritania (West Africa)**: *Physics of the Earth and Planetary Interiors, v. 115*, no. 2, p. 81-100.
Two closely located deep-sea cores taken along the coast of Mauritania contain zones of anomalous NRM directions which fall mainly within the time-spans of published excursions/events for the last 220 kyr. In two cases even reversed polarity is seen. Anomalous directions correspond with strong changes in rockmagnetic properties and in stable oxygen isotope ratios, i.e. glacial/interglacial

transitions. Climatically-controlled changes of the ferromagnetic mineralogy may cause the anomalous NRM directions. Alternatively, geomagnetic field directional changes and climatically-induced mineralogical changes may be caused by a common mechanism.

Hill, M. J., and Shaw, J., 1999, **Palaeointensity results for historic lavas from Mt Etna using microwave demagnetization/remagnetization in a modified Thellier-type experiment**: *Geophysical Journal International, v. 139*, no. 2, p. 583-90.
The microwave palaeointensity technique has been applied to 20 samples of historic lavas from Mt Etna, and with one exception, all samples gave high-quality intensity results. Comparison with a SV model based on direct observatory measurements shows that samples containing a high multidomain (MD) component gave intensity values around 20% lower than expected. Samples with the lowest numbers of MD grains gave field values which, within error, were the same as those for the model, or slightly too high. These deviations are compatible with the cooling rate effect.

Valet, J. P., and Soler, V., 1999, **Magnetic anomalies of lava fields in the Canary Islands. Possible consequences for paleomagnetic records**: *Physics of the Earth and Planetary Interiors, v. 115*, no. 2, p. 109-18.
Measurements of the total magnetic field above the surface of 12 lava flows show directions varying by up to 150° and intensity changes reaching 20%. The deviations are linked to topographic features at the surface of the flows and should persist during emplacement of the next overlying flow. Such effects can thus limit the resolution of paleomagnetic records of detailed geomagnetic features, and the field intensity variations above the flows could explain a significant part of the scatter in paleointensity studies. Samplings performed over large distances within each lava flow would provide the best way to average out the contribution of the anomalies.

Magnetic Microscopy and Spectroscopy

Frenkel, A. I., Cross, J. O., Fanning, D. M., and Robinson, I. K., 1999, **DAFS analysis of magnetite**: *Journal of Synchrotron Radiation, v. 6*, no. 3, p. 332-4.
The mechanism of the structural transformation in Fe_3O_4 during its Verwey transition at 120 K is not completely understood, partly due to the lack of knowledge of the details of the local structure around different Fe atoms in the unit cell. In our experiment, this information was obtained at room temperature using diffraction anomalous fine structure (DAFS) technique which has the ability to separately solve the local structures around the octahedral and tetrahedral sites in the spinel structure of magnetite. An iterative dispersion integral algorithm was used to isolate f ' and f" from the DAFS intensity, and structural information was obtained from f" using standard XAFS analysis methods.

Kim-Ngan, N. T. H., and Soszka, W., 1999, **The Verwey transition of the Fe_3O_4 surface studied by ion scattering spectroscopy**: *Journal of Magnetism and Magnetic Materials, v. 202*, no. 2-3, p. 327-34.
The energy spectra of 5.5 keV He^+, Ne^+, Ar^+ and Kr^+ ions, scattered from a natural surface of a single crystal of magnetite Fe_3O_4, have been measured by ion scattering spectroscopy in the temperature range of 95-300 K. The scattered ion yields $R^+(T)$ show a deep minimum around 120 K followed by a small maximum around 135 K, i.e. around the Verwey transition temperature of the bulk, corresponding to the disorder-order transition of the distribution of Fe^{2+} and Fe^{3+} ions in octahedral sites of the spinel structure. The results are interpreted in terms of the neutralization probability affected by the change of the density of states near the Fermi level, by the change of the electron localization degree as well as of the target material transparency.

Purcell, S. T., and Vu Thien, B., 1999, **Sensitivity of Fresnel projection microscopy for observations of magnetic nanoparticles**: *Journal of Magnetism and Magnetic Materials, v. 198*, no. S0304, p. 01214-1.
Observations of the electron diffraction patterns created by the magnetic leakage fields of individual γFe_2O_3 particles in the 10 nm range have been made with the Fresnel projection electron microscope (FPM) at 200 V. The particle shape and fringes are imaged simultaneously with a resolution of 1 nm. Arguments based on the image formation mechanism by Fresnel diffraction of phase objects are presented which show that the extremely small magnetic fluxes associated with the observed nanoparticles fall within the resolving power of the FPM.

Romero, M., Rincon, J. M., Musik, S., and Kozhukharov, V., 1999, **Mössbauer effect and X-ray distribution function analysis in complex Na_2O-CaO-ZnO-Fe_2O_3-Al_2O_3-SiO_2 glasses and glass-ceramics**: *Materials Research Bulletin, v. 34*, no. 7, p. 1107-15.
Mössbauer spectroscopy at room temperature was carried out to determine the state of iron ions in complex glasses and glass-ceramics in the SiO_2-CaO-ZnO-Na_2O-Fe_2O_3-Al_2O_3 system. Isomer shift values of the glasses suggest that Fe^{3+}; and Fe^{2+} are in tetrahedral and octahedral coordination, respectively. The spectrum of the glass-ceramic shows that about 60 wt% total iron is in the magnetite phase. The Fe^{+3}/Fe^{+2} ratio varies with the total iron oxide content of the glasses, indicating that the vitreous network is more distorted when the iron content is greater.

Wiedenmann, A., Lembke, U., Hoell, A., Muller, R., and Schuppel, W., 1999, **Magnetic nanostructures in a glass ceramic characterized by small angle neutron scattering**: *Nanostructured Materials, v. 12*, p. 5-8.
Nanocrystalline magnetite Fe_3O_4 embedded in a non-magnetic matrix was formed by heat treatment of Ca-Si-B-Fe-oxide glass. Small angle neutron scattering (SANS) revealed a bimodal volume size distribution for the nanocrystalline phase with maxima centred at radii of 2.5 nm and 10 nm, respectively. The magnetic scattering behaviour is characteristic for superparamagnetism of single-domain particles following Langevin statistics. Both fractions of nanocrystals are composed by a superparamagnetic core surrounded by a nonmagnetic surface layer. Magnetisation measurements indicate different thermal variation of the superparamagnetic moments in both fractions of nanocrystals.

Wittborn, J., Rao, K. V., Proksch, R., Revenko, I., Dahlberg, E. D., and Bazylinski, D. A., 1999, **Magnetization reversal observation and manipulation of chains of nanoscale magnetic particles using the magnetic force microscope**: *Nanostructured Materials, v. 12*, p. 5-8.
The magnetization reversal of chains of 40-50 nanometer magnetic particles has been studied using Magnetic Force Microscopy (MFM) in an applied field. The magnetic particles, magnetosomes biomineralized by magnetotactic bacteria, are single crystal Fe_3O_4 with a narrow size distribution. A method for extracting switching field distributions (SFD's) from sets of MFM images of such chains was developed. The coercivity was found to increase with the number of particles in a chain up to 7 or 8 particles and then decrease with increasing number of magnetosomes. After the initial reversal observations, one of the chains was cut into smaller pieces using the MFM-tip, thus producing separated chain segments, which resulted in altered interparticle interactions. Additionally, multiple hysteresis loops were made for the same chain, showing that the field from the tip affects the sample magnetization.

Magnetization Processes

Blanco-Mantecon, M., and O'Grady, K., 1999, **Grain size and blocking distributions in fine particle iron oxide nanoparticles**: *Journal of Magnetism and Magnetic Materials, v. 203*, no. 1-3, p. 50-3.
For three samples of fine-particle magnetite (Fe_3O_4) of different sizes (75, 66, and 58 Å) suspended in a carrier liquid, we compare the physical particle size distribution obtained by TEM with the magnetic particle size. The magnetic particle size characterisation has been determined from the magnetisation curves at room temperature and temperature decay of remanence measurements when the fluids were frozen into the solid state, which give the distribution of energy barriers. We find the existence of a bimodal distribution of particle sizes, confirmed by both the magnetic and non-magnetic studies, which becomes more evident as the particle size becomes smaller.

Bowles, J. A., and Johnson, H. P., 1999, **Behavior of oceanic crustal magnetization at high temperatures: viscous magnetization and the marine magnetic anomaly source layer**: *Geophysical Research Letters, v. 26*, no. 15, p. 2279-82.
Although the source layer for marine magnetic anomalies has been assumed to be the extrusive basalts of uppermost ocean crust, studies indicate that lower crustal rocks may also contribute. To evaluate the temperature at which magnetization of crustal rocks achieves long-term stability, we undertook high-temperature VRM (viscous

remanent magnetization) experiments on samples of basalt, dike and gabbroic sections. Samples were heated at temperature intervals up to Tc, while a magnetic field was applied for periods between 6 hours and 28 days. The dike and gabbro samples achieve maximum VRM acquisition near 250° C, well below the Tc of 580° C. The basalt sample shows a peak at 68° C, also well below Tc. Results of this pilot study indicate that the critical isotherm for stable magnetization acquisition is defined by the VRM behavior of the specific crustal section.

Keller, R., and Schmidbauer, E., 1999, **Magnetic hysteresis properties and rotational hysteresis losses of synthetic stress-controlled titanomagnetite ($Fe_{2.4}Ti_{0.6}O_4$) particles. I. Magnetic hysteresis properties**: *Geophysical Journal International, v. 138*, no. 2, p. 319-33.
Synthetic TM60 particles of a few selected grain sizes were subjected to different treatments, affecting the microcrystalline state, and an attempt was made to interpret the experimental magnetic parameters from room temperature up to the Curie point in light of theoretical models that include the influence of the microcrystalline structure. The present study encompasses results regarding magnetic hysteresis properties and rotational hysteresis losses. For PSD and MD particles, a crucial point is the pinning of domain walls at lattice defects.

Papusoi, C., Jr., 1999, **The particle interaction effects in the field-cooled and zero-field-cooled magnetization processes**: *Journal of Magnetism and Magnetic Materials, v. 195*, no. 3, p. 708-32.
Particle interactions affect FC and ZFC magnetization curves by 1) the anisotropy effect, referring to the increase of the temperature T_{MAX}, corresponding to the ZFC curve maximum, with increasing concentration, and 2) the mean-field effect, referring to the flattening of both the FC and ZFC magnetization curves with increasing sample demagnetizing factor, without altering T_{MAX} in the low applied field limit. We show that the anisotropy effect of interactions is due to not only an increase of the particle anisotropy with increasing sample volume concentration, but also to a temperature-dependent interaction field distribution due to the local non-homogeneity of the particle dispersion. The proposed model is able to recover the experimental FC and ZFC initial susceptibility curves for various concentrations of γ-Fe_2O_3 nanoparticle systems.

Wasilewski, P., and Kletetschka, G., 1999, **Lodestone: nature's only permanent magnet-what it is and how it gets charged**: *Geophysical Research Letters, v. 26*, no. 15, p. 2275-8.
Magnetite and titanomagnetite exhibit magnetic properties which are attributable to the micro-structures developed during oxidation and exsolution: all magnetite iron ores which are lodestones contain maghemite. Magnetite, titanomagnetite and metals all have REM values (NRM/SIRM ratios)<0.05. Fulgarite samples obtained from the Smithsonian Institution have REM values ranging from 0.45 to 0.92. The REM value serves as a witness parameter to the magnetic fields associated with the lightning bolt. The magnetic field associated with lightning can be revealed from an isothermal remanent acquisition curve.

Worm, H. U., 1999, **Time-dependent IRM: a new technique for magnetic granulometry**: *Geophysical Research Letters, v. 26*, no. 16, p. 2557-60.
The intensities of isothermal remanent magnetizations (IRM) acquired in 0.01 s and 10 s can differ by more than an order of magnitude depending on field strength and sample composition. For 15 samples containing magnetite, titanomagnetite, maghemite, hematite or pyrrhotite of distinct grain sizes, ranging from superparamagnetic (SP) through stable single domain (SSD) to multidomain (MD), the IRM acquisition has been measured for the two time constants. In addition, the viscous decay following IRM acquisition within 2000 s has been determined. In low fields (≤10 mT) the IRM(10s)/IRM(0.01s) ratios range from 1.03 for MD grains up to >20 for SP/SSD grains. For fields larger than the coercivity of remanence the IRM ratio approaches unity for all samples. Viscous decay after IRM acquisition is much larger for samples containing SP grains than for SSD and MD grains. Hence, a viscous decay parameter $S_0=(IRM_{16}-IRM_t)/\log(t/t_0)$ normalized by the saturation remanence can serve as an alternative to the frequency dependence of susceptibility, the commonly used proxy for SP grains. In fact, it may be more sensitive because remanences cannot be masked by para- or diamagnetic contributions and IRMs can be measured reliably on weakly magnetic sediments.

Modeling and Theory

Fabian, K., and Hubert, A., 1999, **Shape-induced pseudo-single-domain remanence**: *Geophysical Journal International, v. 138*, no. 3, p. 717-26.
Models of uniaxial hard magnetic particles show that irregularly shaped grains possess a considerable equilibrium remanence due to domain imbalance. This remanence decreases approximately as L^{-1} with grain size L and is very stable with respect to alternating field and thermal demagnetization. It is therefore likely to be a major source of pseudo-single-domain remanence in rocks. Using the methods of domain theory, the range of possible remanences in irregularly shaped uniaxial particles with less than five domains is investigated. Even for slightly asymmetric particle geometries the remanence decreases monotonically with grain size. Most two-domain remanences lie above 0.3 M_s. The behaviour of the domain imbalance moments seems to be largely independent of details of the shape asymmetry. Since domain imbalance is a global equilibrium remanence, local remanences due to wall pinning effects can be superimposed without destroying it. This can explain the fact that the remanence of pseudo-single-domain particles appears to be a mixture of independent single- and multidomain-like components.

Synthesis and Properties of Magnetic Minerals

Anantharaman, M. R., Reijne, S., Jacobs, J. P., Brongersma, H. H., Smits, R. H. H., and Seshan, K., 1999, **Preferential exposure of certain crystallographic planes on the surface of spinel ferrites: a study by LEIS on polycrystalline spinel ferrite surfaces**: *Journal of Materials Science, v. 34*, no. 17, p. 4279-83.
Spinel ferrites are commercially important because of their excellent magnetic and catalytic properties. Study of selected spinel ferrites by low energy ion scattering (LEIS) has revealed atomic scale information on their surfaces, showing that the octahedral sites are preferentially exposed on the surfaces. The probable planes exposed are D(110) or B(111).

Morales, M. P., Andres-Verges, M., Veintemillas-Verdaguer, S., Montero, M. I., and Serna, C. J., 1999, **Structural effects on the magnetic properties of γ-Fe_2O_3 nanoparticles**: *Journal of Magnetism and Magnetic Materials, v. 203*, no. 1-3, p. 146-8.
Structural and magnetic properties of γ-Fe_2O_3 have been studied in spherical nanoparticles ranging from 3 to 15 nm with a narrow particle size distribution. Partial cationic order is observed for particles larger than 10 nm in diameter while the smallest ones are disordered. All magnetic properties measured showed a strong dependence on the average crystallite size. Saturation magnetization was found to decrease linearly with decreasing crystallite size in the ordered samples. However, a stronger decrease was observed in the disordered samples, suggesting that both surface and structural characteristics are needed in order to explain the magnetic properties of nanoparticles.

Wells, M. A., Fitzpatrick, R. W., Gilkes, R. J., and Dobson, J., 1999, **Magnetic properties of metal-substituted haematite**: *Geophysical Journal International, v. 138*, no. 2, p. 571-80.
Mineral and isothermal magnetic properties of Al-, Mn- and Ni-substituted haematites generally resemble those of single-domain (SD) particles. Al acts as a paramagnetic dilutent, decreasing χ. Mn and Ni increased χ, which could be associated with enhancement of the spin canting effect. Al substitution leads to development of smaller crystallites and high stability of SIRM800 to demagnetization. Data indicate that parameters involving unsaturated, partial SIRM should be used with caution in magnetic studies of soils and sediments.

Yogo, T., Nakamura, T., Sakamoto, W., and Hirano, S., 1999, **Synthesis of magnetic particle/organic hybrid from metalorganic compounds**: *Journal of Materials Research, v. 14*, no. 7, p. 2855-60.
A nanocrystalline magnetic particle/oligomer hybrid was successfully synthesized by polymerization of iron(III) 3-allylacetylacetonate followed by in situ hydrolysis. Crystalline particles of approximately 10 nm were found to be dispersed in the oligomeric matrix and were identified as iron oxide spinel by X-ray diffraction analysis and electron diffraction.

...Fields

continued from page 1

water-cooled resistive (Bitter-type) magnets, ranging from 15 to 20 tesla. One of the latter gained wide attention for the Nijmegen lab in 1996, when it was used to levitate a live frog. (Frogs, like other animals, consist mostly of water, which is diamagnetic; frogs therefore become magnetized in the direction opposite that of the applied field, and are repelled by the field

The celebrated levitated frog of Nijmagen Laboratory

gradient at the mouth of the coil). The frog was reported to have suffered no distress as a result of the experiment.

The apex of steady magnetic field technology is represented by the hybrid magnet systems, which combine a superconductive outer magnet and a cooled resistive inner coil. The Nijmegen-II hybrid system can generate a total field of 30.4 tesla in a 32-mm room-temperature bore. The US National High Magnetic Field Lab (NHMFL) in Tallahassee, Florida, has a 45 tesla hybrid system that produces the strongest steady magnetic field on earth (approximately one million times the geomagnetic field magnitude).

The fun really begins with pulsed magnets, which generate enormous fields of brief duration. Short pulse lengths limit the resistive heat loss, enabling transient currents and fields that, with longer application, would melt the coil. The NHMFL pulsed-field facility at Los Alamos maintains two categories of instruments: non-destructive and destructive magnets. In the non-destructive magnets, the enormous stresses generated during a pulse approach, but do not exceed, the strength of the materials from which the magnet is constructed. Material strength and time are thus the limiting factors; non-destructive pulsed fields of 60 tesla can currently be applied for durations of up to 2 seconds, and 100 tesla for 20 ms, without catastrophic failure.

Destructive pulsed magnet systems attain greater fields by ignoring the limitations of material strength: they are designed to explode with every pulse. Pulse duration is limited to a few microseconds, after which the magnet self-destructs. For example, a capacitor-driven single-turn coil design at Los Alamos generates a 4-microsecond pulse of 250 tesla.

Still higher transient fields can be produced by still more drastic technologies. The highest experimental magnetic fields are achieved by explosive flux compression: chemical explosives are detonated around a magnet as it is pulsed, and the magnetic field is "compressed" and concentrated by the convergent flow of hot ionized gases. Fields exceeding 850 tesla have been generated in microsecond pulses. This appears to qualify as the grand champion magnetic field on planet Earth.

Which begs the question: what about extraterrestrial magnetic fields? We know that the necessary conditions for generation of the geomagnetic field involve vigorous, thermally- and/or chemically-driven convection in an electrically-conductive region (the outer core). These conditions undoubtedly exist in at least some of the other planets in our solar system, but a more interesting candidate for very strong magnetic fields is the sun itself, and other stars.

Magnetism in Stars

First a bit of backgound; let's start with sunspots. Detailed Chinese records of sunspot activity extend back more than two millennia, but in Europe observations did not begin until the Renaissance, when Galileo and others began making telescopic observations around 1610. A number of interesting phenomena were soon recognized: sunspots are transient features on the solar surface, lasting on average a few days; they occur in narrow belts of latitude within about 30° of the solar equator; and they rotate in unison across the face of the sun, indicating the 27-day rotation of the sun itself about its axis. The rotation period, as recognized by Richard Carrington in the 1850's, actually varies significantly with latitude, from 25 days at the equator to 35 days in the polar regions.

Transient fields approaching 1000 tesla are generated by explosive compression of magnetic flux at the National High Magnetic Field Lab in Los Alamos.

Very few sunspots occurred during the latter half of the 1600's (a period now known as the Maunder minimum). Observation continued during the 18th and 19th centuries, and in 1843 Heinrich Schwabe pointed out that, based on his own observations, sunspot occurrence exhibits a strong 10-year cycle. Rudolf Wolf confirmed the cyclic nature of sunspot activity in historical records (and revised the average period to a bit more than 11 years). Later Carrington observed that sunspot latitudes varied systematically through the 11-year cycle, occurring primarily near ±30° at the beginning of a cycle, and at then at progressively lower latitudes. (This observation is also known as Spoerer's Law, and usually illustrated by means of the "Maunder butterfly" diagram.)

But what, exactly, are sunspots? The answer began to emerge with the telescopic spectral studies of Hale in the early 1900's, which showed a characteristic duplication, or splitting, of Frauenhofer absorption lines. Hale recognized this splitting as the Zeeman effect, the spectral shift imposed on emission or absorption lines by a strong magnetic field. Pieter Zeeman had discovered in 1886 that the line wavelengths are shifted in direct proportion to magnetic field strength, and Hale was thereby able to measure the magnetic fields associated with sunspots, which he found reached nearly 0.5 tesla. He concluded that sunspots were magnetic storms.

Further, he found that spots tend to occur in pairs of opposite polarity, i.e., a north (+) and a south (-) magnetic pole. Moreover, he recognized a hemispheric regularity in the disposition of these pairs, with (+) invariably to the east of (-) in the northern hemisphere, and the reverse in the southern hemisphere.

All of these observations fit neatly together in the standard solar dynamo model. Start with a weak, dominantly poloidal field. The poloidal field lines are trapped in the electrically-conductive outer layers of the sun, and the shearing due to differential rotation eventually twists the field into an intense toroidal configuration. The strong toroidal field is carried outward by convection, and occasionally a "flux bundle" erupts through the solar surface, producing a sunspot pair with oppositely directed (outward/inward) fields. As sunspot activity builds to a maximum, the strong toroidal field is dissipated by this flux expulsion, first at latitudes near ±30°, where the shearing is most pronounced, and thence equatorward. Ultimately the field "short-circuits" across the equator,

Hale, George Ellery

b. June 29, 1868, Chicago;
d. Feb 21, 1938, Pasadena

Hale discovered the magnetic fields associated with sunspots in 1908, when he recognized the spectral line splitting in his spectroheliographic observations as a manifestation of the Zeeman effect. More generally Hale is remembered for the development of astronomical observatories and instruments. In Chicago he organized the Kenwood Observatory around 1890, and it was there that he invented the spectroheliograph. He established the Yerkes Observatory at Williams Bay, WI, where he served as director and built a 40-inch refractor, which is the largest of that type ever built. Later he organized the observatories on Mount Wilson and Mount Palomar, the latter of which houses the 200-inch Hale telescope.

returning to a weak, dominantly poloidal configuration, with a polarity opposite that of the initial field.

Thus, in contrast to the Earth, where field reversals occur at very irregular intervals typically of the order of millions of years, the solar magnetic field reverses its polarity in a regular cycle, on average every 11.4 years. As in the geodynamo, the interaction of weak poloidal and stronger toroidal fields appears to play a critical role.

But to return to the subject at hand, even the toroidal field of the sun is only about half a tesla. This exceeds the geomagnetic field by a factor of 100, but still pales in comparison to artificially-generated fields. However, let us not give up; the sun is an ordinary main-sequence star, and there are many more exotic species in the astronomical bestiary where we can look for stronger fields.

Take neutron stars, for example. These are the staggeringly dense, imploded remnant cores of rather massive stars that have cataclysmically exploded as supernovas. The protons and electrons of ordinary matter collapse under the violence, fusing into neutrons, which are packed together so tightly that the neutron star has a bulk density very close to that of its constituent neutrons. How dense is that? Neutron stars have a mass comparable to the sun's, crammed into a diameter of 20 km; the density is an inconceivable 10^{17} kg per cubic meter. A sand-grain-sized speck of this material would tip the scales at around half a million tons.

Equally astonishing is the rate of rotation: a "typical" neutron star takes about *one second* to complete a rotation around its axis. This is deduced from the pulsations in radiation received from these stars (which are also known as *pulsars*, due to this distinctive behavior). The pulsations are belived to be linked to immensely powerful magnetic fields, dipolar and distinctly non-coaxial with the pulsar spin axis. Intense beams of radiation are emitted from the magnetic polar regions, and the rotation of the neutron star sweeps the radiation beams around like lighthouse beacons. There is also a pulsar wind of charged particles, like the solar wind, through which the pulsar gradually loses rotational energy; all known pulsars are observed to be slowing down.

The rotation period and its rate of change are the essential information that make it possible to calculate the magnetic field. The fastest pulsars have periods of about a millisecond and spindown rates of about 10^{-20} sec/sec, yielding calculated magnetic fields of about 10^4 tesla, about 10 times greater than the best pulsed fields on Earth. Another power of ten would bring us to the lethal level of 10^5 tesla, which, it is estimated, would produce fatal molecular distortions. "Ordinary" pulsars boldly go *way* beyond that, to fields of around 10^8 tesla.

Many millisecond and ordinary pulsars are known. In contrast, the slowest pulsars, with periods around 10 seconds, are relatively rare: only four or five have been identified. The magnetic fields of these are monstrous, approaching 10^{11} tesla, and for this reason they are known as "magnetars". To say that such fields are beyond our powers of imagination would be an understatement. A magnetar at the distance of the moon would immediately erase all of the magnetically-stored information on and in the Earth. (It would undoubtedly also produce a variety of other inconvenient effects).

These slow pulsars have other unusual features as well, presumed to be related to their enormous magnetic fields. For example, they pulse primarily in the highly-energetic x-ray portion of the electromagnetic spectrum, in contrast to the radio-wave to gamma-wave radiation characteristic of the other pulsars. But perhaps their most remarkable behavioral characteristic is gamma-ray bursts. The *soft-gamma repeaters* occasionally emit colossal bursts of soft (low-frequency) gamma rays. One of them (SGR1900+14), on August 27 1998, bathed the Earth in enough radiation to cause detectable changes in the ionization state of our atmosphere, despite its great distance (20,000 light years). These gamma-ray bursts are thought to originate in "starquakes". Like the destructive pulse magnets on earth, the immense magnetic fields of the slow pulsars exert titanic stresses on their solid crusts. Ruptures are spectacularly energetic: translated into the familiar Richter scale, the SGR quakes register a distinctly unfamiliar magnitude of 20.

The range of naturally and artificially produced magnetic fields in the the observable universe thus spans a remarkable 18 orders of magnitude. This is so large that it is exceptionally difficult to conceive. However, to put matters into a different perspective, even the gargantuan fields of soft-gamma repeaters are vanishingly *small* compared to the largest theoretically possible field: 10^{45} - 10^{49} tesla (for which I will not even attempt to supply an adjective!). This limit is imposed, in a sense, by the material strength of empty space. According to theorist Robert Duncan of the University of Texas (co-author of the magnetar hypothesis), in fields approaching 10^{49} tesla space itself suffers a quantum-mechanical breakdown, producing magnetic monopoles.

Of course, it may be some time before we can test *that* theory.

Field, T	*Source or Effect*
$2x10^{-7}$	typical laboratory "field-free space"
$5x10^{-5}$	geomagnetic field at Earth's surface
$2x10^{-4}$	perturbs computer monitor display
$2x10^{-3}$	erases credit cards, magnetic tapes, etc.
$5x10^{-3}$	toroidal field in Earth's core
$3x10^{-2}$	erases floppy disks
$6x10^{-2}$	lightning bolt (30,000 Amps, 10 cm distance)
$3x10^{-1}$	refrigerator magnets
$5x10^{-1}$	sunspots
$1x10^{0}$	typical lab electromagnets, MRI systems
$1x10^{1}$	levitates frogs
$4x10^{1}$	strongest steady laboratory fields (hybrid magnets)
$1x10^{2}$	maximum field of ordinary stars
$1x10^{2}$	strongest nondestructive experimental pulsed fields
$1x10^{3}$	maximum experimental pulsed field
$1x10^{4}$	field of fast (millisecond) pulsars
$1x10^{5}$	estimated lethal field
$1x10^{8}$	typical field of "ordinary" neutron stars (radio pulsars)
$1x10^{11}$	"magnetars" (soft-gamma repeaters)

Fields

continued on page 8...

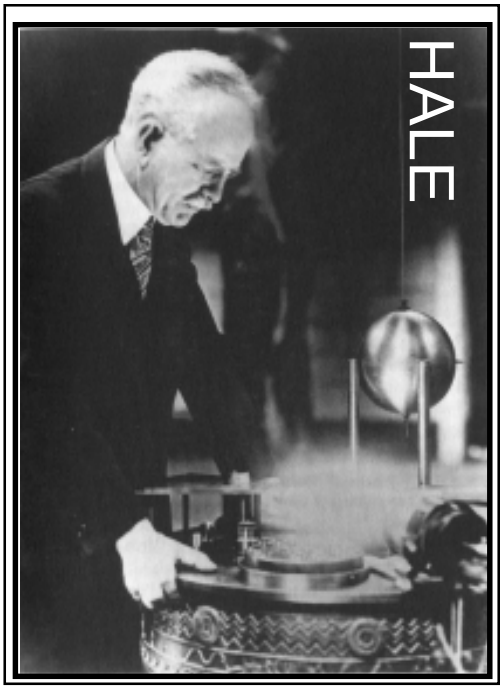

Collector's Series #14

Hale and his solar spectrograph.
from *Pauper & Prince: Ritchey, Hale & Big American Telecopes,* by Donald Easterbrock, 1993, University of Arizona Press

The *Institute for Rock Magnetism* is dedicated to providing state-of-the-art facilities and technical expertise free of charge to any interested researcher who applies and is accepted as a Visiting Fellow. Short proposals are accepted semi-annually in spring and fall for work to be done in a 10-day period during the following half year. Shorter, less formal visits are arranged on an individual basis through the Facilities Manager.

The *IRM* staff consists of **Subir Banerjee**, Professor/Director; **Bruce Moskowitz**, Associate Professor/ Associate Director; **Jim Marvin**, Senior Scientist; **Mike Jackson**, Senior Scientist and Facility Manager, and **Peat Solheid**, Scientist.

Funding for the *IRM* is provided by the **W. M. Keck Foundation**, the **National Science Foundation**, and the **University of Minnesota**.

The *IRM Quarterly* is published four times a year by the staff of the *IRM*. If you or someone you know would like to be on our mailing list, if you have something you would like to contribute (*e.g.*, titles plus abstracts of papers in press), or if you have any suggestions to improve the newsletter, please notify the editor:

Mike Jackson
Institute for Rock Magnetism
University of Minnesota
291 Shepherd Laboratories
100 Union Street S. E.
Minneapolis, MN 55455Ð0128
phone: (612) 624-5274
fax: (612) 625-7502
e-mail: irm@geolab.geo.umn.edu
www.geo.umn.edu/orgs/irm/irm.html

I R M

Institute for Rock Magnetism

...Fields

continued from page 7

For more information:

Duncan, R. C., 'Magnetars', soft-gamma repeaters & very strong magnetic fields, http://solomon.as.utexas.edu/~duncan/magnetar.html

Hale, G. E., The Earth and Sun as magnets, *Smithsonian Institution Ann. Rept.*, 145-158, 1913.

NASA MSFC Vector Magnetograph, http://wwwssl.msfc.nasa.gov/ssl/pad/solar/maggraph.htm

High Field Magnet Laboratory (U. of Nijmegen), http://www-hfml.sci.kun.nl/hfml/

National High Magnetic Field Laboratory (Florida St. U, U. of Florida, Los Alamos National Lab), http://www.nhmfl.gov/

Sonett, C. P., M. S. Giampapa, and M. S. Matthews, eds., *The Sun in Time*, University of Arizona Press, 1991.

Winn, J. N., The life of a neutron star, *Sky & Telescope, 98 (1),* 30-38, 1999.

Zhang, K., and D. R. Fearn, How strong is the invisible component of the magnetic field in the Earth's core?, *Geophys. Res. Lett., 20,* 2083-2086, 1993.

The IRM Quarterly

University of Minnesota
291 Shepherd Laboratories
100 Union Street S. E.
Minneapolis, MN 55455Ð0128
phone: (612) 624-5274
fax: (612) 625-7502
e-mail: irm@geolab.geo.umn.edu
www.geo.umn.edu/orgs/irm/irm.html